

Comparative Analysis of the Influence of Different Preparation Methods on the Properties of TEMPO-Oxidized Bacterial Cellulose Powder Films

Dieter Rahmadiawan^{a,b}, Shih-Chen Shi^a, Hairul Abral^{c,d}, Mohammad Khalid Ilham^c,
Eni Sugiarti^e, Ahmad Novi Muslimin^{e,f}, R.A Ilyas^g, Remon Lapisa^b,
and Nandy Setiadi Djaya Putra^h

^aDepartment of Mechanical Engineering, National Cheng Kung University (NCKU), Tainan, Taiwan; ^bDepartment of Mechanical Engineering, Universitas Negeri Padang, Padang, Sumatera Barat, Indonesia; ^cLaboratory of Nanoscience and Technology, Department of Mechanical Engineering, Andalas University, Padang, Sumatera Barat, Indonesia; ^dResearch Collaboration Center for Nanocellulose, BRIN-Andalas University, Padang, Indonesia; ^eLaboratory of High-Temperature Coating, Research Center for Physics Indonesian Institute of Sciences (LIPI) Serpong, Banten, Indonesia; ^fWeaponry Technology Study Program, Defense Technology Faculty, Indonesia Defense University, Bogor, Indonesia; ^gSchool of Chemical and Energy Engineering, Faculty of Engineering, Universiti Teknologi Malaysia, Johor Bahru, Malaysia; ^hHeat Transfer Laboratory, Department of Mechanical Engineering, Universitas Indonesia, Depok, Indonesia

ABSTRACT

The preparation method of cellulose films plays a vital role in their properties. This work aims to characterize 2, 2, 6, 6-tetramethylpiperidine-1-oxyl (TEMPO)-oxidized bacterial cellulose powder (TOBCP) films prepared with three different methods (casting, boiling-casting, and boiling-vacuum). It is found that film by casting (CT film) shows the best electrical properties. A light-emitting diode (LED) in a direct current circuit connected to the CT film glows the most brightly. However, this film had lower tensile strength and thermal stability than films from boiling and boiling-vacuum techniques. The boiling-vacuum film presents the most compact fiber structure and the highest tensile and thermal properties. This film also shows the lowest electrical properties and the dimmest LED light. These results demonstrate the TOBCP properties from different methods that can be used to prepare film with desirable properties.

摘要

纤维素薄膜的制备方法对其性能起着至关重要的作用。本工作旨在表征采用三种不同方法（流延、沸腾流延和沸腾真空）制备的2, 2, 6, 6-四甲基哌啶-1-氧基（TEMPO）氧化细菌纤维素粉末（TOBCP）薄膜。研究发现，流延薄膜（CT薄膜）具有最佳的电学性能。连接到CT胶片的直流电路中的发光二极管（LED）发光最亮。然而，该膜的拉伸强度和热稳定性低于沸腾和沸腾真空技术的膜。沸腾真空膜呈现出最紧凑的纤维结构和最高的拉伸和热性能。该薄膜还显示出最低的电性能和最暗淡的LED光。这些结果证明了不同方法的TOBCP性能，可用于制备具有所需性能的膜。

KEYWORDS



Bacterial cellulose; electrical properties; conductivity; light-emitting diode; ultrasonication


关键字

细菌纤维素; 电气特性; 电导率; 发光二极管; 超声处理

Introduction

In these modern days, while ‘semiconductor and synthetic’ technology is often preferable for its conductivity and robustness, it also presents disadvantages such as environmental impact and resource depletion (Fauza et al. 2023; Tun et al. 2023). Nature provides many types of natural fibers

CONTACT Hairul Abral  habral@yahoo.com  Laboratory of Nanoscience and Technology, Department of Mechanical Engineering, Andalas University, Padang, Sumatera Barat 25163, Indonesia

 Supplemental data for this article can be accessed online at <https://doi.org/10.1080/15440478.2023.2301386>

© 2024 The Author(s). Published with license by Taylor & Francis Group, LLC.

This is an Open Access article distributed under the terms of the Creative Commons Attribution License (<http://creativecommons.org/licenses/by/4.0/>), which permits unrestricted use, distribution, and reproduction in any medium, provided the original work is properly cited. The terms on which this article has been published allow the posting of the Accepted Manuscript in a repository by the author(s) or with their consent.

that can be used in various applications (Liu et al. 2022; Moradi, Alihosseini, and Ghadami 2023; Sharif et al. 2021; Rahmadiawan et al. 2022). The natural fibers consist of cellulose, lignin, and hemicellulose (Liu et al. 2020). However, the cellulose from the wood is obtained by the natural fiber extraction process using chemicals that are harmful to the environment. Environmentally friendly cellulose nanofiber can be gained by *Acetobacter xylinum* bacterium, i.e., wet BC pellicle (Meldawati et al. 2023). The pellicle consists of long cellulose nanofibers interconnected in a three-dimensional structure (de Souza et al. 2023). Because of excellent BC properties: high purity and crystallinity, excellent mechanical and thermal properties, and biocompatibility, many nanofibers from bacterial cellulose have been used as basic materials for various purposes (Charoenrak et al. 2023; Fatima et al. 2021; Gabilondo et al. 2021; Izakura, Koga, and Uetani 2021; Rahmadiawan et al. 2023; Xi et al. 2023).

Large-scale fabrication of BC pellicles faces significant obstacles. For instance, long-term storage of wet BC pellicles needs a substantial amount of room. This deficiency restricts the potential for more sophisticated applications. In previous research, the raw material for BC was obtained by employing a mechanical process on the wet BC pellicle before further processing it into other products (Wu and Cheng 2017; Ummartyotin et al. 2012). Recently, we established a novel technique for obtaining BC powder by drying and crushing the wet pellicle (Rahmadiawan et al. 2023). The benefit of this method is that huge amounts of dry BC powder may be manufactured and kept in a simple, airtight container before use. The BC powder may then be delivered on demand to make other cellulose-based films. Nevertheless, films produced utilizing the dry BC powder alone, with no further processing, have poor tensile characteristics (Abral et al. 2022).

The manner of processing has a significant impact on the qualities of cellulose-based films (Hou, Xu, and Li 2018; Orr, Sonekan, and Shofner 2020). Different chemical or mechanical treatment procedures might result in films with distinct characteristics (Celebi and Kurt 2015). TEMPO-oxidized bacterial cellulose films have exhibited strong ionic conductivity, which correlates to their large porosity and electrolyte storage capacity and carry electrical current (Huang et al. 2020; Jiang et al. 2015). Using the solution casting technique, AM Abdel-Karim et al. created a conductive film from TEMPO bagasse fibers (Abdel-Karim, Salama, and Hassan 2018). Additionally, the ultrasonic treatment of dry BC powder might alter the characteristics of cellulose films. Ultrasonication has recently been shown to increase electrical characteristics and transparency (Aguilera et al. 2020; Baskut 2022; Rahmadiawan et al. 2023; Siljander et al. 2018). However, the fabrication and characterization of TOBCP powder-based films from a variety of preparation methods remain restricted. The preparation method affects the properties and production time of the TOBCP film when it is mass-produced. For this reason, various alternative ways are needed to find TOBCP film with minimal costs and sufficient characteristics. These factors motivated us to investigate the produced TOBCP film by different methods, with the expectation of designing a more optimal film.

The first research related to BC film was in 2010 (Saibuatong and Phisalaphong 2010). As far as the author is aware, until now, there is no commercialized paper that originated from pure BC. The literature states that the total time from invention to widespread commercialization ranges from 19 to 70 years, with a mean time of 45 years (Hanna, Gross, and Gross 2015). Therefore, much still needs to be done. In order to meet commercial demand, it requires lengthy processes, including the design of large-scale, semi-continuous, and continuous production (Lin et al. 2013). In all cases, the primary objective is to achieve the maximum production of BC film with the optimal preparation method and suitable properties for food packaging applications.

Herein, we characterized BC powder films made by casting, boiling-casting, and vacuum-boiling techniques. To the author's knowledge, no works on the application of the approach have been recorded.

It is hypothesized that the characteristics of the BC film will vary depending on which of these three methods are used to prepare it. Due to the smallest number of hydroxyl functional groups, the vacuum film has the worst electrical conductivity but the best mechanical properties. The vacuum method increases the likelihood of inter-hydrogen and intra-hydrogen bond

formation, which leads to a decrease in free electrons and, ultimately, a decrease in conductivity. As a result of the high free charges present on oxygen atoms with high electronegativity, the casting film is capable of producing the most electricity. In the meantime, the boiled film's electrical and mechanical properties will be intermediate between those of the casting and vacuum methods. Additionally, the mechanical, thermal, and transparent properties of the films were reported. This work may shed light on approaching or getting closer to commercialized BC for various applications.

Materials and methods

Materials

Wet BC pellicles used were purchased locally (Padang, Indonesia). 2,2,6,6-Tetramethylpiperidine-1-oxyl (TEMPO) was obtained from Sigma-Aldrich Co, USA. Sodium hypochlorite (NaClO), sodium bromide (NaBr), and sodium hydroxide (NaOH) were purchased from Sigma-Aldrich Co, USA.

Preparation of TEMPO treated BC film

Preparation of BC powder: A BC pellicle (35 cm x 25 cm x 0.5 cm), as shown in [Figure 1a](#), was treated using 10% NaOH solution. After 48 h, it was neutralized and cleaned until pH 7. Then, the wet pellicle was disintegrated using a Maspion blender at 12,000 rpm for 1 h. It was dried for 24 hours at 70°C in a drying oven. To produce BC powder, the dried pellicle was crushed using a grinder at 3500 rpm for one hour. Then, it was filtered using sieves with mesh sizes of 60, 100, and 200. ([Figure 1b](#)).

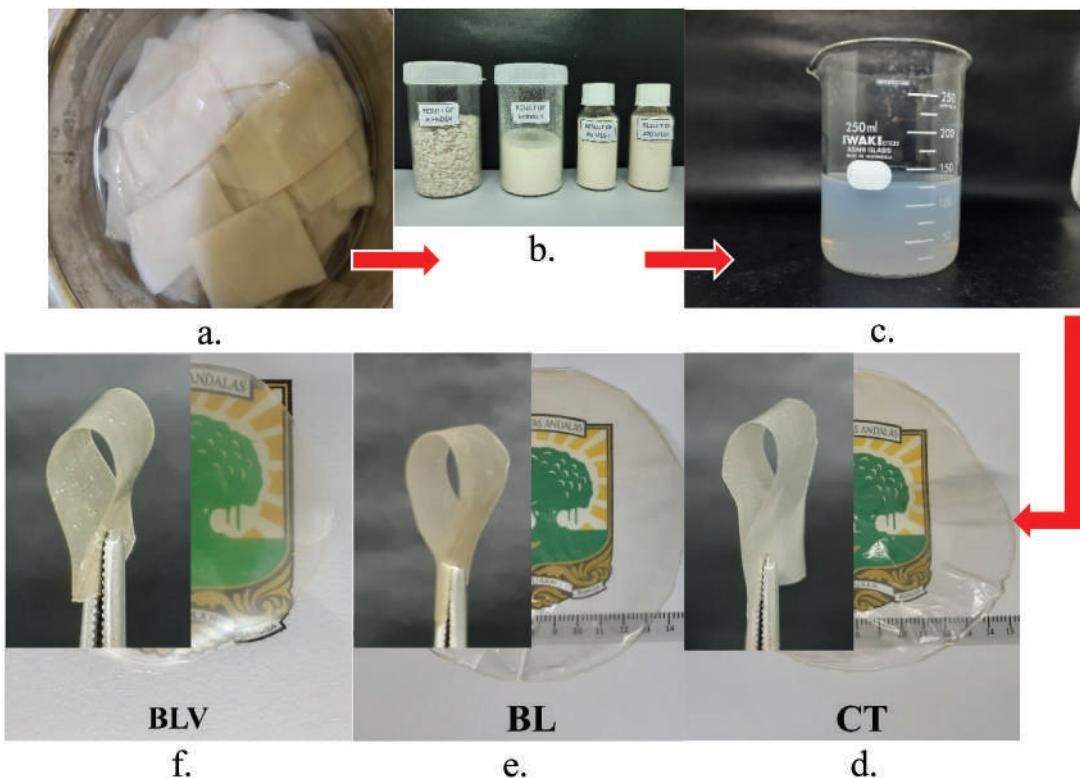


Figure 1. (a) BC pellicles, (b) BC powders, (c) treated BC suspension from various ultrasound energy, (d) CT film, (e) BL film, and (f) BLV film.

Preparation of TOBCP suspension: The BC oxidizing treatment by TEMPO is similar to our previous works (Rahmadiawan et al. 2023). The mixture of BC powder, NaClO, and NaBr was stirred using a hot plate magnetic for 20 min at 50°C. About 0.5 M NaOH was added to the mixture to neutralize its pH. The process was repeated to prepare three suspensions treated with CT, BL, and BLV techniques.

Preparation of CT, BL, and BLV films: Each TOBCP suspension was centrifuged for 30 min at 3000 rpm. After the TOBC nanofiber was fully sedimented, the water in the tube was removed slowly and replaced with new distilled water. After the pH reached 7, the suspension was treated with a high-shear homogenizer (WiseTis Homogenizer HG-15D DAIHAN Scientific Co., Ltd. from Gangwon-do, Korea) at 6000 rpm for 30 minutes. Hereafter, an FS-1200N ultrasonication homogenizer operating at 480 W was operated for 20 min. Then, using the CT, BL, and BLV procedures, these three sonicated suspensions were created. CT films were made by pouring the sonicated suspension directly onto a Teflon plate (12 cm diameter). Meanwhile, the BL film was produced by boiling the suspension at 100°C for 4 h and then casting it on the Teflon plate. For the BLV film, the sonicated suspension was boiled at 100°C for 4 h, and then the water was removed by filtering through a Buchner funnel fitted with a filter paper (0.45 µm porosity, 47 mm diameter) connected to a vacuum pump. All wet BC films from the three methods were dried using a drying oven at 50°C for 48 h. All films were stored in a desiccator with 50% relative humidity at room temperature.

Characterization

FESEM observation

A JEOL model JFIB 4610 SEM (10 kV accelerating current and 8 mA probe current) was utilized to investigate the surface morphology of the sample. The samples of the BC film were placed on the FESEM sample stub and coated with carbon and gold to lower the electron charge.

Film opacity

A spectrophotometer model Shimadzu UV 1800 was used to gauge the films opacity. Samples that were produced and placed in the spectrophotometer were rectangles shape (1 cm x 2.5 cm). The ASTM D 1003–00 test procedure was used as reference for determining haze and luminous transmittance in transparent polymers. The range of the absorbance spectrum was between 200 and 800 nm. The area beneath the absorbance spectrum was used to calculate the film's opacity. This opacity test was repeated three times for each sample.

FTIR

FTIR of the sample was characterized using a PerkinElmer Frontier equipment. The dried samples were formed into a sheet film and scanned at a frequency range of 4000–400 cm⁻¹ at 4 cm⁻¹ resolution.

X-ray diffraction

X-ray diffraction testing was performed using PANalytical Xpert PRO (Philips Analytical, Netherlands) at 25°C, 40 kV, and 30 mA with CuKα radiation (λ = 0.154). The samples were scanned from 2θ = 5° to 90°. The percentage of crystallinity index (CI) was measured using Equation 1 (Segal et al. 1958):

$$CI(\%) = \frac{(I_{200} - I_{am})}{I_{200}} \times 100 \quad (1)$$

where I_{200} , and I_{am} are the cellulose I peak intensity and the peak of the amorphous fraction respectively.

Thermal stability

Shimadzu DTG-60 was used to evaluate samples' thermal stability. The apparatus was set up with a nitrogen flow rate of 50 mL/min, and temperature pace of 20°C/min.

Tensile properties

The COM-TEN 95T Series 5K (Pinellas Park, USA) tensile test (5 mm/min speed, at room temperature) was utilized to analyze the samples' tensile characteristics. The testing complies with ASTM D 638 type V standard. All samples were kept in a desiccator at 25°C for 48 hours with a relative humidity of 50% before the test.

Electrical properties

Before testing electrical properties, the samples were stored in a 50% RH desiccator for 48 h. A four-point probe (JG, M-3) was used to measure the electrical resistance (R) of films at room temperature. The R was measured five times per sample in the same direction, and the results were averaged. The Equations 2 and 3 were used to calculate the resistivity and conductivity values:

$$\rho = \frac{\pi t}{\ln 2} R \quad (2)$$

$$\sigma = \frac{1}{\rho} \quad (3)$$

where ρ is resistivity (Ωcm), σ conductivity (S/cm), t film thickness (cm), R Resistance (Ω) of measured films.

Statistical analysis

The calculation of the significance of film properties for three different methods was carried out using variance (ANOVA). Duncan's multiple-range test was used to examine differences were significant at $p \leq 0.05$.

Results and discussions

BC powder and suspension, a BC film appearance, and transmittance value

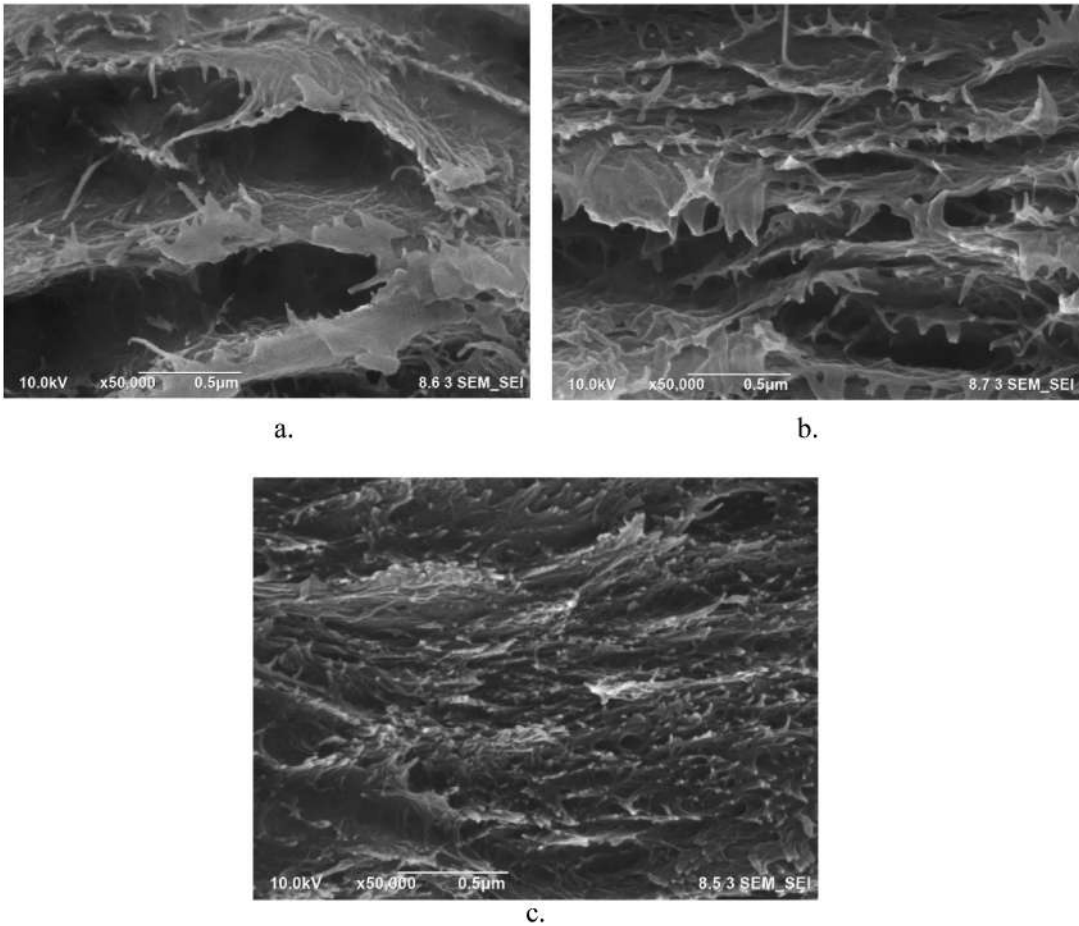
Figure 1a shows wet pellicles before being crushed to obtain dry BC powder (Figure 1b). All films transparency and thickness are shown in Table 1. Meanwhile, Figure 1c presents a sonicated and TEMPO treated BC powder suspension in order to prepare the CT (Figure 1d), BL (Figure 1e), and BLV films (Figure 1f). Each film had good transparency and consistent thickness. The object under the film was still clearly observable. After testing the transmittance value from 200–800 nm wavelength, using the BLV method, the transparency of the sample increases (Figure 1e), and the light transmittance at 650 nm shifts to 62.24% (Figure 1g and Table 1). The BLV film was the most transparent due to the lowest light reflection passing through the film. This increased transparency is because boiling and vacuuming assisted in forming intra- and interlinking hydrogen bonds resulting in highly crystalline domains (Song et al. 2018). As a result, the film with high crystallinity consisting of densely packed cellulose molecules reflects light small enough (Nogi et al. 2009). These results are in good

Table 1. Transmittance at 650 nm and thickness of all films.

Samples	Transmittance (%) at 650 nm	Thickness (μm)
CT	61.43	354
BL	62.20	352
BLV	62.24	357

Table 2. Crystallinity index (CI) from Figure 4, and the T_{max} from Figure 5.

Samples	CI (%) of (200) plane	T_{max} ($^{\circ}$ C)
CT	88.58	317.3
BL	87.88	320.1
BLV	93.25	324.9

**Figure 2.** FESEM fracture surface morphology of (a) CT, (b) BL, and (c) BLV samples.

agreement with the XRD pattern (Figure 4), displaying a higher CI value of the BLV film (93.25%) than the CT film (88.58%) (Table 2).

FESEM morphology

The fracture surface FESEM morphology in the cross-section of the tensile specimens produced from three different methods is displayed in Figure 2. The CT sample (Figure 2a) contains a sparse fiber configuration confirming a low compact structure. Boiling or boiling-vacuuming caused the BC nanofibers to get denser, the amount of voids decreased, and the neatly organized layers to become more noticeable (Figures 2b). The most compact nanofiber structures are observable in BLV film, as shown in Figure 2c. This sample had a larger fiber surface contact area than the CT, increasing cross-

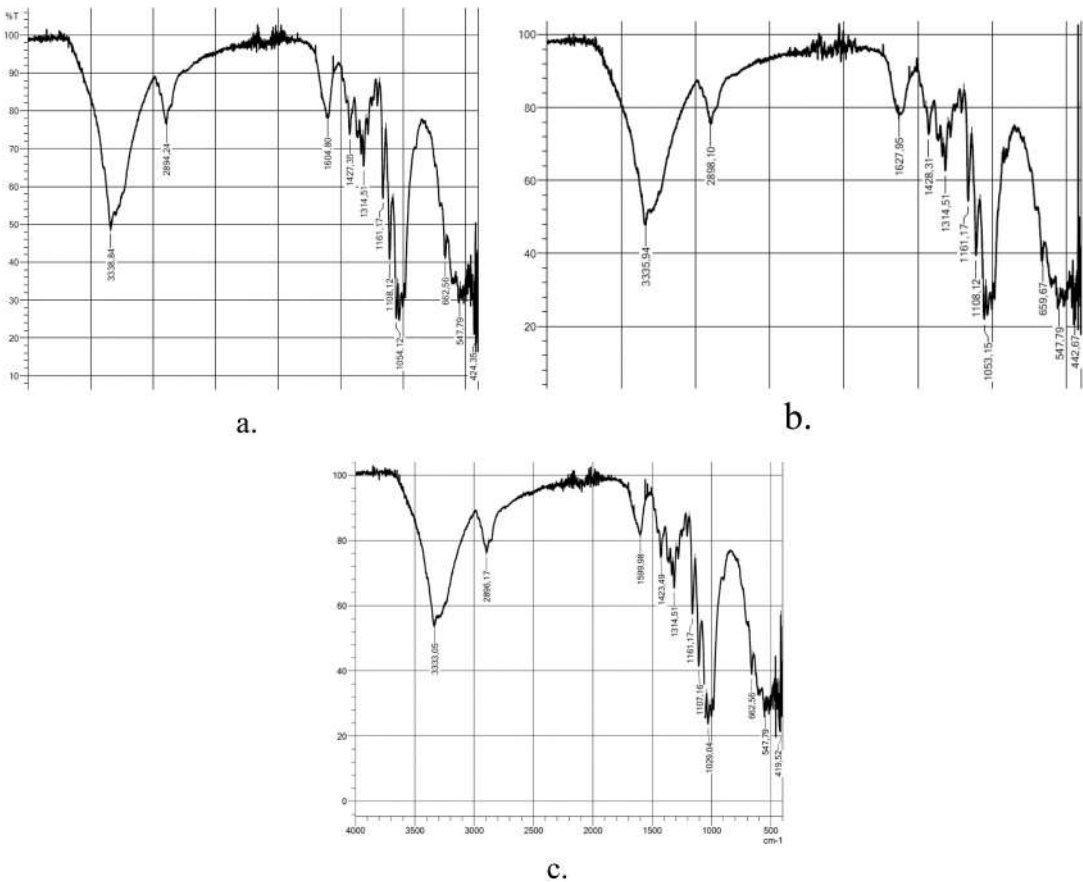


Figure 3. FTIR patterns of (a) CT, (b) BL, and (c) BLV samples.

linking hydrogen bonds between polymer chains. This finding is consistent with the FTIR curves (Figure 3), showing a shift of the peak position of OH- stretching vibrations at around 3339 cm^{-1} to lower wavenumber after boiling and boiling-vacuum.

FTIR spectra

FTIR spectroscopy was used to observe the effect of different methods on the characterization of the cellulose functional groups (Ilyas, Sapuan, and Ishak 2018). Figure 3 shows the FTIR spectra for BC films prepared using casting (Figure 3a), casting-boiling (Figure 3b), and boiling-vacuum methods (Figure 3c). The FTIR pattern of films is broadly similar, indicating that these three different methods did not affect the chemical structure of BC. A similar finding agrees with previous works (Zhang et al. 2019). However, using the various sample preparations shifted the wavenumbers and intensities of the spectrum peaks. These results may be attributed to changes in cellulosic structure (Kondo 1997). This structural change is consistent with the XRD pattern (Figure 4). The CT film presents peak positions at 3339 cm^{-1} and 1604 cm^{-1} , corresponding to OH- stretching vibrations and OH-bending of adsorbed water, respectively (Qu et al. 2021). This film had the lowest T value (48%) at 3339 cm^{-1} , resulting from the largest free hydroxyl functional group fraction (Abral et al. 2020). After preparing with BL and BLV methods, this peak position moved to 3336 cm^{-1} (Figure 3b) and 3333 cm^{-1} (Figure 3c). The T value for the BLV film was 54%, increased by about 13% compared to the CT. These shifted values correspond to the increased interlinking of hydrogen bonding between the cellulose molecules (Abral

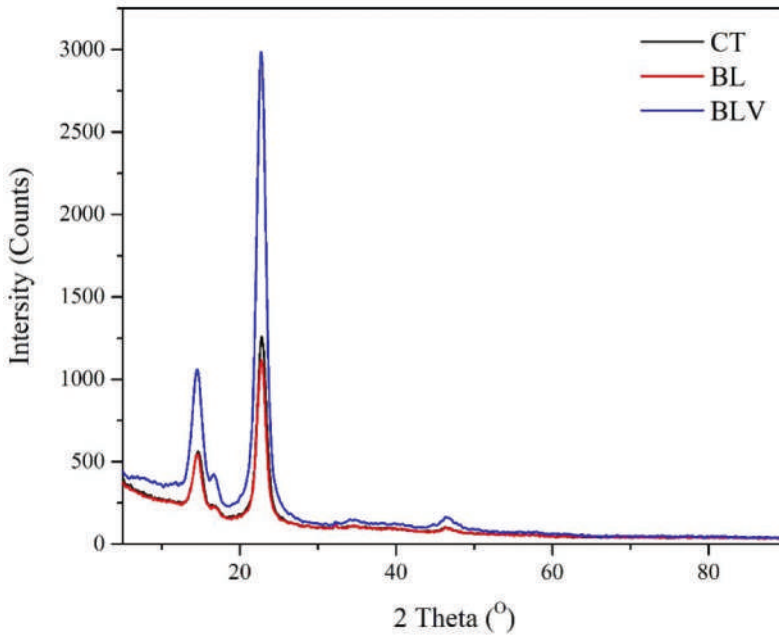


Figure 4. X-ray diffraction patterns of films.

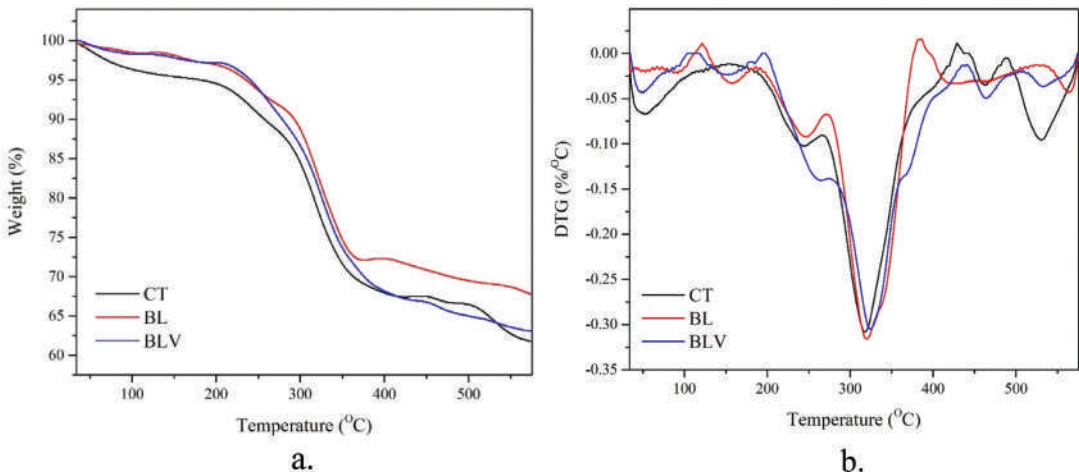


Figure 5. (a) TGA, and (b) DTA curve for CT, BL, and BLV films.

et al. 2022). Thus, the number of interlinked fiber molecules increases, decreasing the free OH groups available in the BL and BLV samples (Udoetok, Wilson, and Headley 2018). A similar finding agrees with previous work (Zhang et al. 2019).

X-ray diffraction

Figure 4 shows the X-ray diffraction pattern of BC films from various treatments. The figure presents that all BC films have typical cellulose I diffraction patterns with two main peaks at about $2\theta = 22.7^\circ$ and 14.6° . This result agrees with the previously reported diffraction pattern (Lu et al. 2014). The non-

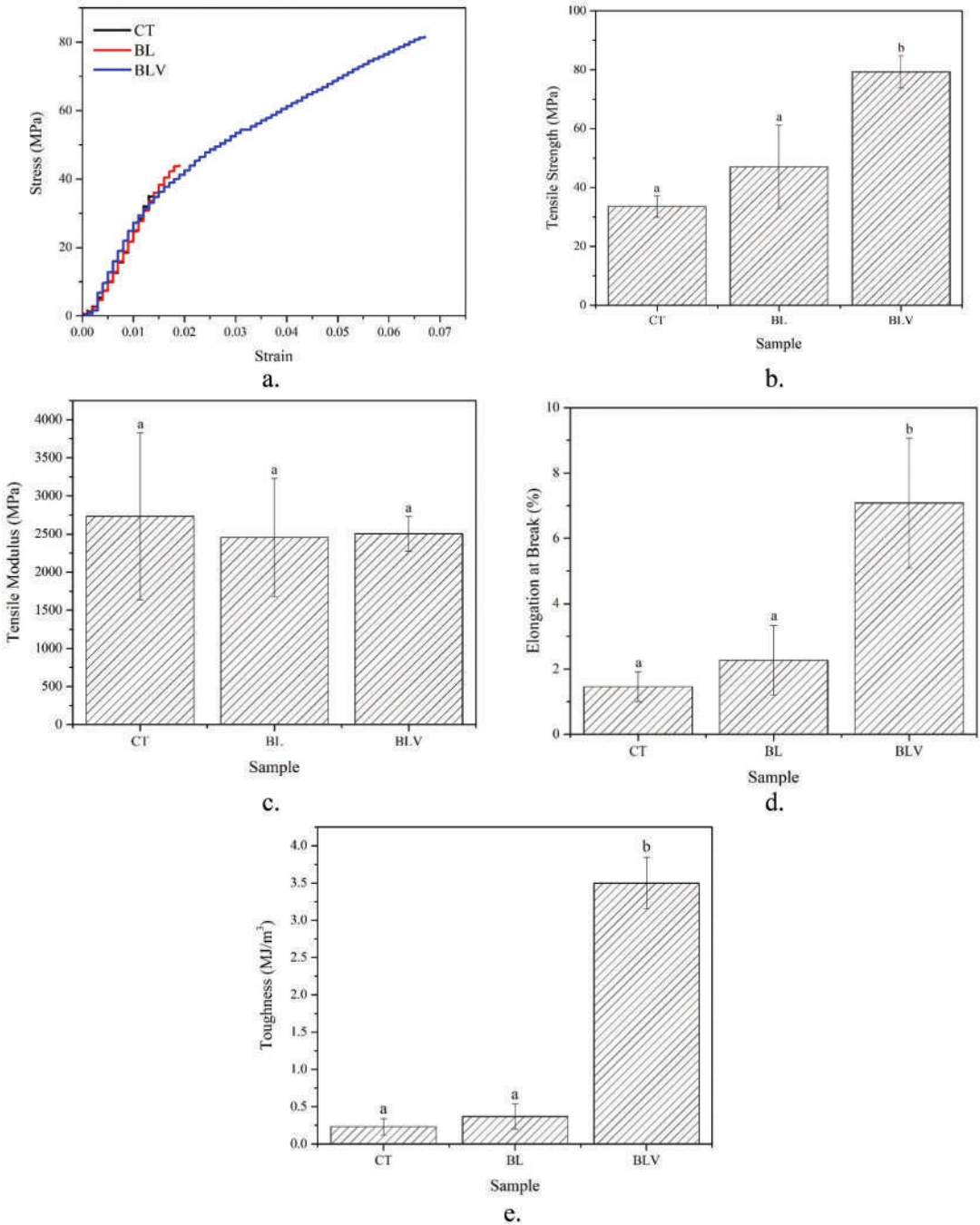


Figure 6. Average tensile test for all films (a), TS (b), TM (c), EB (d), and TN (e).

vacuumed films (CT and BL) had low CI (Table 2) due to low crystal fraction. These films displayed similar CI values (88.58% for the CT and 87.88% for the BL). Also, the height of their spectrum peaks was lower than the BLV film. After using the boiling-vacuum technique, the CI shifted to 93.25%, increasing by 5.3% compared to the CT film. This is probably due to the increment of interlinking hydrogen bonding resulting in the reordering of the crystal structures (Nakagaito, Nogi, and Yano

2010Dinesh and Kandasubramanian 2022). This result is in good agreement with the more compact fiber structure (FESEM morphology in Figure 1c) and higher tensile strength (Figure 6b) of the BLV than the CT film.

Thermal properties

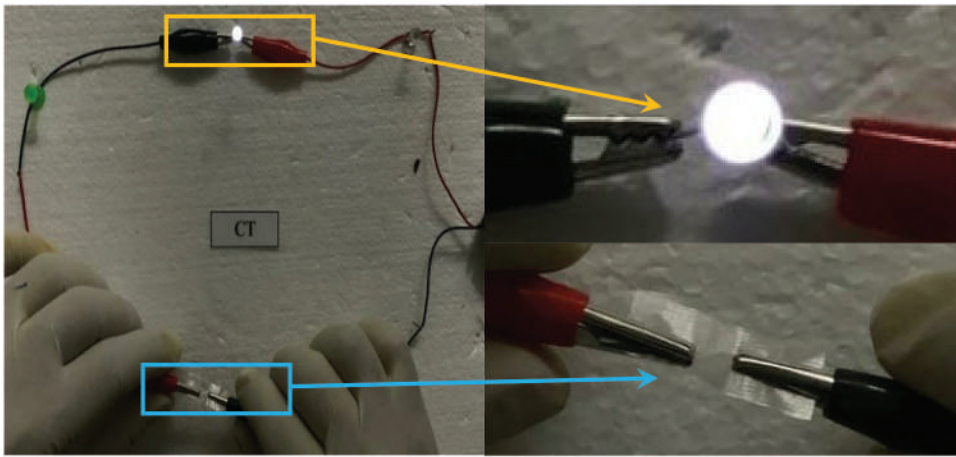
Figure 5 displays the thermal properties of CT, BL, and BLV films. All samples lost their initial weight in the temperature range of 60–150°C due to the evaporation of the absorbed water (Badshah et al. 2018). Because of the highest water content, the CT film presents the highest weight loss (Putra A et al. 2021). On heating in the temperature range of 300–420°C, a considerable weight loss was associated with the decomposition of cellulose (Wu and Cheng 2017). The CT film had lower thermal stability than the BL and BLV ones. This result can be observed at the maximum decomposition temperature (T_{max}). T_{max} for the CT sample was 317.3°C, shifted to 320.1°C, and 324.9°C after boiling-casting and boiling-vacuum treatments, respectively. This shift confirms that the thermal energy required for pyrolysis of BLV cellulose nanofibers was higher than that of other films. This phenomenon is because boiling-vacuum treatment of the BLV film increased the crosslinking polymer, thus strengthening bonds between the cellulose chains; consequently, the cellulose decomposition slowed. That is why the heat resistance of BLV films has increased. This improved thermal stability agrees with the increased crystal index of the BLV film (see Table 2) and previous work (Yousefi et al. 2013). Finally, the third weight loss occurred above 420°C due to charcoal decomposition.

Tensile properties

Figure 6a shows the stress-strain curves of films. The CT film has low tensile strength and strain values resulting from a low fiber density ratio and compatibility. After the boiling-vacuum treatment, the stress-strain curve of films increased significantly due to increases in the compactness of the fiber structure. This BLV film undergoes great plastic deformation and has the largest area under the stress-strain curve. Figures 6b, 6c, 6d, and 6e show the average values of the tensile strength (TS), tensile modulus (TM), elongation at break (EB), and toughness (TN) for all films, respectively. Using the casting-boiling technique, the TS, EB, and TN values were low, and the film was brittle. In contrast, with the BLV method, these tensile properties increased significantly. Compared to the CT film, the TS, EB, and TN of the BLV films were 79.29 MPa, 7.08%, and 3.50 MJ/m³; which increased by 137%, 388%, and 1417%, respectively. The significantly improved tensile properties correspond to increased hydrogen bond crosslinking (Kondo, 1997) and more compact cellulose structures of the BLV film (Figure 2c) than the CT and BL films. This phenomenon agrees with the higher CI value (Table 2) and a peak position shift for the O–H stretching vibration to a lower value (Figure 3) after boiling and vacuum treatments. This high TS and EB properties of BLV is higher than those in our prior work (43.2 MPa), which is almost 100% improvement compared to this work (Rahmadiawan, Abral, Kotodeli, et al., 2023). It is possible that the boiling and vacuum method could contribute to incremental progress in producing BC films for commercialized products. It is estimated that a commercialized product using this method could be achievable in the next 19 years (Hanna et al., 2015).

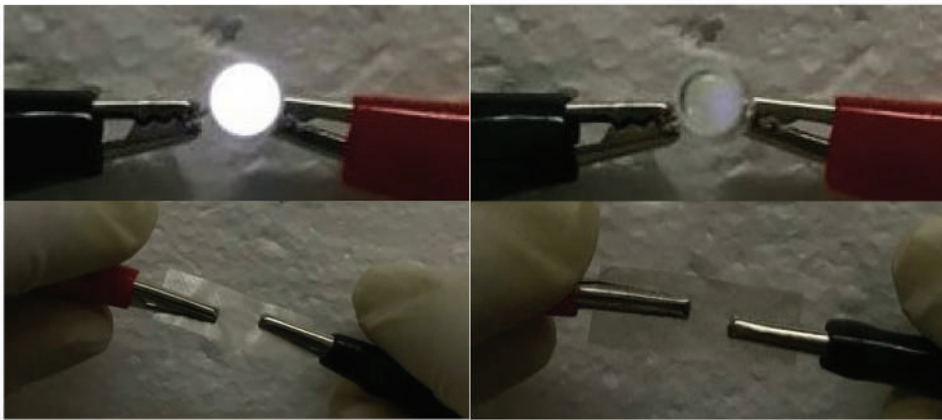
Electrical properties

A simple direct current (DC) circuit (Figure 7a) consisting of 3 V LEDs connected with films and a 9 V battery can be seen in the supplemental videos (Videos S1–S3). Figures 7b–d present the light intensity of 3 V LEDs connected with CT, BL, and BLV films with a thickness of 21 mm, 34 mm, and 53 mm, respectively. The LED linked to the CT film shone the brightest (Figure 7b) due to the lowest electrical resistance ($R = 36.12 \text{ k}\Omega$) and the best electrical conductivity ($s = 2.93 \text{ mS/cm}$), as shown in Figure 7e. The high electrical conductivity can be attributed to the sonication process. Sonication creates a high-porosity structure in materials by breaking down cellulose fibers into smaller fragments or causing the



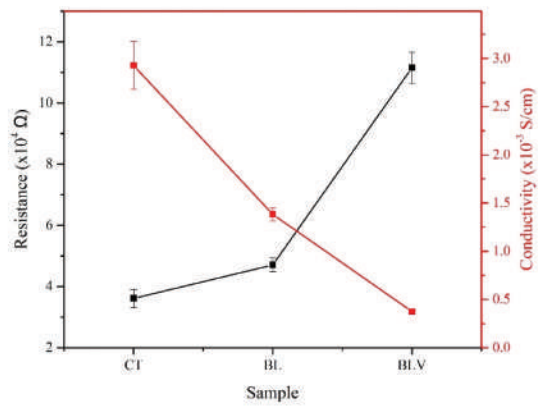
a.

b.



c.

d.



e.

Figure 7. (a) A DC circuit linked to the CT film. Intensities of LED lights connected with (b) CT, (c) BL, and (d) BLV films. (e) Electrical resistance and conductivity of the CT, BL, and BLV films at 50% RH and room temperature.

formation of voids and pores within the film (Ybañez and Camacho 2021). This will increase the film's porosity and result in a network of open spaces within the film. More pathways and channels are available in a film with higher porosity. These pathways facilitate the movement of electrons, allowing them to move more easily through the interconnected network of pores and free OH groups. This discussion is consistent with Figure 2 (Sheng et al. 2020). Furthermore, a highly porous film structure can lead to an increased surface area. This larger surface area potentially provides more sites for electron interaction and transport (Mihrianyan et al. 2008).

After connecting the BL and BLV films, however, light brightness decreases (Figures 7c,d). The σ value for the BL film was 1.38 mS/cm, a decrease of 52.8%. A significant drop occurred in the BLV film, showing $\sigma = 0.37$ mS/cm; representing an 87.2% decrease compared to the CT film. Consistent with the previous statement, this decrease can be attributed to a reduction in the electron transfer medium, i.e., the free hydroxyl groups, resulting from an increase in inter-hydrogen and intra-hydrogen bonds (Abdel-Karim, Salama, and Hassan 2018). Thus, the number of the porosity fraction and dimension (see Figure 2) and free hydroxyl groups (see Figure 3) reduced and consequently increased the electrical resistance of the BL and BLV films. *Previous work also presented a similar agreement showing a lower ionic conductivity of the BC films due to a reduction of its porosity (Jiang et al. 2015).*

Conclusions

This work has successfully studied the effect of three different methods of thin-film preparation on the properties of sonicated and TEMPO-oxidized BC films. The BC film prepared via the CT method had the best conductivity (2.93×10^{-3} S/cm) but the lowest mechanical and thermal properties. In contrast, the boiling-vacuum treatment improved tensile properties and heat resistance. But using this method, the σ value of the BLV film decreased by 87.22% compared to the CT film. This finding is because the BLV treatment reduced the ion transfer medium, i.e., free hydroxyl groups and nanopores. The results of this study have improved the understanding profoundly of the film preparation effect on its properties obtained. These techniques have great potential for preparing TOBCP powder-based films in food packaging application with selectable properties depending on the desired conditions.

Acknowledgments

This work was supported by the Universitas Andalas for supporting research funding with project name Riset Kolaborasi Indonesia (Skema A), number : 3/UN16.19/PT.01.03/PRK-RKI Skema A (Host)/2023.

Disclosure statement

No potential conflict of interest was reported by the authors.

Funding

Universitas Andalas granted Professor Hairul Abral funding for the project named Riset Kolaborasi Indonesia (Skema A).

Author's contribution

Dieter Rahmadiawan : Writing – Original Draft, Formal Analysis, Visualization

Shih-Chen Shi : Writing – Review & Editing, Validation

Hairul Abral : Writing – Review & Editing, Supervision, Funding Acquisition, Conceptualization

Mohamad Khalid Ilham: Investigation

Eni Sugiarti : Resources
Ahmad Novi Muslimin: Resources, Investigation
A Ilyas : Resources, Validation
Remon Lapisa : Writing – Review & Editing
Nandi Setiadi Djaya Putra: Writing – Review & Editing

Consent to participate

All authors contribute and participate in the work carried out in this paper.

Consent for publication

The authors of this paper agree to publish this work in the Journal of Natural Fibers.

Ethical approval

All authors agree and accept Ethics approval.

References

- Abdel-Karim, A. M., A. H. Salama, and M. L. Hassan. 2018. "Electrical Conductivity and Dielectric Properties of Nanofibrillated Cellulose Thin Films from Bagasse." *Journal of Physical Organic Chemistry* 31 (9): 1–9. <https://doi.org/10.1002/poc.3851>.
- Abral, H., J. Ariksha, M. Mahardika, D. Handayani, I. Aminah, N. Sandrawati, A. B. Pratama, N. Fajri, S. M. Sapuan, and R. A. Ilyas. 2020. "Transparent and Antimicrobial Cellulose Film from Ginger Nanofiber." *Food Hydrocolloids* 98:105266. <https://doi.org/10.1016/j.foodhyd.2019.105266>.
- Abral, H., A. Kurniawan, D. Rahmadiawan, D. Handayani, E. Sugiarti, and A. N. Muslimin. 2022. "Highly Antimicrobial and Strong Cellulose-Based Biocomposite Film Prepared with Bacterial Cellulose Powders, Uncaria Gambir, and Ultrasonication Treatment." *International Journal of Biological Macromolecules* 208 (March): 88–96. <https://doi.org/10.1016/j.ijbiomac.2022.02.154>.
- Aguilera, L., N. Fagundes, A. D. Melo, B. Bandeira, F. X. Nobre, J. Anglada-Rivera, J. P. Silva, J. Pérez de la Cruz, and Y. Leyet. 2020. "Influence of Sonication Time on the Structure and Electrical Properties of Na₂Ti₆O₁₃ Ceramics: An Approach Applying the Mott-Schottky Model." *Ceramics International* 46 (7): 8706–8710. <https://doi.org/10.1016/j.ceramint.2019.12.106>.
- Badshah, M., H. Ullah, A. R. Khan, S. Khan, J. K. Park, and T. Khan. 2018. "Surface Modification and Evaluation of Bacterial Cellulose for Drug Delivery." *International Journal of Biological Macromolecules* 113:526–533. <https://doi.org/10.1016/j.ijbiomac.2018.02.135>.
- Baskut, S. 2022. "Effects of Adding GPLs Dispersed at Different Sonication Times on the Thermal and Electrical Conductivities of Spark Plasma Sintered Silicon Carbide." *Materials Chemistry and Physics* 287 (May): 126230. <https://doi.org/10.1016/j.matchemphys.2022.126230>.
- Celebi, H., and A. Kurt. 2015. "Effects of Processing on the Properties of Chitosan/Cellulose Nanocrystal Films." *Carbohydrate Polymers* 133:284–293. <https://doi.org/10.1016/j.carbpol.2015.07.007>.
- Charoenrak, S., S. Charumanee, P. Sirisa-Ard, S. Bovonsombut, L. Kumdhithaihutsawakul, S. Kiatkarun, W. Pathom-Aree, T. Chitov, and S. Bovonsombut. 2023. "Nanobacterial Cellulose from Kombucha Fermentation as a Potential Protective Carrier of Lactobacillus Plantarum Under Simulated Gastrointestinal Tract Conditions." *Polymers*, 15(6), 1356. <https://doi.org/10.3390/polym15061356>
- de Souza, T. C., J. D. P. de Amorim, C. J. G. da Silva Junior, A. D. M. de Medeiros, A. F. de Santana Costa, G. M. Vinhas, and L. A. Sarubbo. 2023. "Magnetic Bacterial Cellulose Biopolymers: Production and Potential Applications in the Electronics Sector." *Polymers* 15 (4): 1–15. <https://doi.org/10.3390/polym15040853>.
- Dinesh, G., and B. Kandasubramanian. 2022. "Fabrication of transparent paper devices from nanocellulose fiber." *Materials Chemistry and Physics* 281 (May 2021): 125707. <https://doi.org/10.1016/j.matchemphys.2022.125707>.
- Fatima, T., R. Jolly, M. R. Wani, G. G. H. A. Shadab, and M. Shakir. 2021. "Exploring the bone regeneration potential of bio-fabricated nano-titania reinforced polyvinyl alcohol/nano-cellulose based composite film." *Results in Materials* 12 (October): 100240. <https://doi.org/10.1016/j.rinma.2021.100240>.
- Fauza, A. N., F. Qalbina, H. Nurdin, A. Ambiyar, and R. Refdinal. 2023. "The Influence of Processing Temperature on the Mechanical Properties of Recycled PET Fibers." *Teknomekanik* 6 (1): 21–28. <https://doi.org/10.24036/teknomekanik.v6i1.21472>.

- Gabilondo, N., A. E. Alon, N. Gabilondo, A. Eceiza, and A. Retegi. 2021. "A Review of Bacterial Cellulose: Sustainable Production from Agricultural Waste and Applications in Various Fields." *Cellulose* 4 (13): 8229–8253. <https://doi.org/10.1007/s10570-021-04020-4>.
- Hanna, R., R. Gross, and R. Gross. 2015. Innovation Timelines from Invention to Maturity. *Technology and Policy Assessment Innovation Timelines from Invention to Maturity* (December). UKERC. <https://doi.org/10.13140/RG.2.1.5016.4560>
- Hou, M., M. Xu, and B. Li. 2018. "Enhanced Electrical Conductivity of Cellulose Nanofiber/Graphene Composite Paper with a Sandwich Structure." *ACS Sustainable Chemistry and Engineering* 6 (3): 2983–2990. <https://doi.org/10.1021/acssuschemeng.7b02683>.
- Huang, C., H. Ji, Y. Yang, B. Guo, L. Luo, Z. Meng, L. Fan, and J. Xu. 2020. "TEMPO-Oxidized Bacterial Cellulose Nanofiber Membranes as High-Performance Separators for Lithium-Ion Batteries." *Carbohydrate Polymers* 230:230. <https://doi.org/10.1016/j.carbpol.2019.115570>.
- Ilyas, R. A., S. M. Sapuan, and M. R. Ishak. 2018. "Isolation and Characterization of Nanocrystalline Cellulose from Sugar Palm Fibres (*Arenga Pinnata*)." *Carbohydrate Polymers* 181:1038–1051. <https://doi.org/10.1016/j.carbpol.2017.11.045>
- Izakura, S., H. Koga, and K. Uetani. 2021. "Humidity-Responsive Thermal Conduction Properties of Bacterial Cellulose Films." *Cellulose* 28 (9): 5363–5372. <https://doi.org/10.1007/s10570-021-03888-6>.
- Jiang, F., L. Yin, Q. Yu, C. Zhong, and J. Zhang. 2015. "Bacterial Cellulose Nanofibrous Membrane as Thermal Stable Separator for Lithium-Ion Batteries." *Journal of Power Sources* 279:21–27. <https://doi.org/10.1016/j.jpowsour.2014.12.090>.
- Kondo, T. 1997. "The Assignment of IR Absorption Bands Due to Free Hydroxyl Groups in Cellulose." *CELLULOSE* 4 (4): 281–292.
- Lin, S. P., I. Loira Calvar, J. M. Catchmark, J. R. Liu, A. Demirci, and K. C. Cheng. 2013. "Biosynthesis, Production and Applications of Bacterial Cellulose." *Cellulose* 20 (5): 2191–2219. <https://doi.org/10.1007/s10570-013-9994-3>.
- Liu, W., H. Du, M. Zhang, K. Liu, H. Liu, H. Xie, X. Zhang, and C. Si. 2020. "Bacterial Cellulose-Based Composite Scaffolds for Biomedical Applications: A Review." *ACS Sustainable Chemistry and Engineering* 8 (20): 7536–7562. <https://doi.org/10.1021/acssuschemeng.0c00125>.
- Liu, W., K. Liu, H. Du, T. Zheng, N. Zhang, T. Xu, B. Pang, X. Zhang, C. Si, and K. Zhang. 2022. "Cellulose Nanopaper: Fabrication, Functionalization, and Applications." *Nano-Micro Letters* 14 (1): 1–27. <https://doi.org/10.1007/s40820-022-00849-x>.
- Lu, Q., L. Tang, F. Lin, S. Wang, Y. Chen, X. Chen, and B. Huang. 2014. "Preparation and Characterization of Cellulose Nanocrystals via Ultrasonication-Assisted FeCl₃-Catalyzed Hydrolysis." *Cellulose* 21 (5): 3497–3506. <https://doi.org/10.1007/s10570-014-0376-2>.
- Meldawati, K., S. Ilyas, T. Tamrin, I. Radecka, S. Swingler, A. Gupta, A. G. Stamboulis, and S. Gea. 2023. "Bioactive Bacterial Cellulose Wound Dressings for Burns with Collagen in-Situ and Chitosan ex-Situ Impregnation." *International Journal of Biological Macromolecules* 230 (September 2022): 123118. <https://doi.org/10.1016/j.ijbioacc.2022.123118>.
- Mihriyan, A., L. Nyholm, A. E. Garcia Bennett, and M. Strømme. 2008. "A Novel High Specific Surface Area Conducting Paper Material Composed of Polypyrrole and Cladophora Cellulose." *Journal of Physical Chemistry B* 112 (39): 12249–12255. <https://doi.org/10.1021/jp805123w>.
- Moradi, Z., A. Alihosseini, and A. Ghadami. 2023. "Adsorption Removal of Arsenic from Aqueous Solution by Carboxy Methyl Cellulose(cmc) Modified with Montmorillonite." *Results in Materials* 17 (December 2022): 100378. <https://doi.org/10.1016/j.rinma.2023.100378>.
- Nakagaito, A. N., M. Nogi, and H. Yano. 2010. "Displays from Transparent Films of Natural Nanofibers." *MRS Bulletin* 35 (3): 214–218. <https://doi.org/10.1557/mrs2010.654>.
- Nogi, M., S. Iwamoto, A. N. Nakagaito, and H. Yano. 2009. "Optically Transparent Nanofiber Paper." *Advanced Materials* 21 (16): 1595–1598. <https://doi.org/10.1002/adma.200803174>.
- Orr, M. P., A. Sonekan, and M. L. Shofner. 2020. "Effect of Processing Method on Cellulose Nanocrystal/polyethylene-Co-Vinyl Alcohol Composites." *Polymer Engineering and Science* 60 (12): 2979–2990. <https://doi.org/10.1002/pen.25527>.
- Putra, A., R. P. Sari, E. Nasra, E. Yuniarti, and A. Amran. 2021. "Bacterial cellulose-rambutan leaf extract (*Nephelium lappaceum* L.) composite: preparation and characterization." *Journal of Physics. Conference Series* 1876 (1): 012027. <https://doi.org/10.1088/1742-6596/1876/1/012027>.
- Qu, R., M. Tang, Y. Wang, D. Li, and L. Wang. 2021. "TEMPO-Oxidized Cellulose Fibers from Wheat Straw: Effect of Ultrasonic Pretreatment and Concentration on Structure and Rheological Properties of Suspensions." *Carbohydrate Polymers* 255 (November 2020): 117386. <https://doi.org/10.1016/j.carbpol.2020.117386>.
- Rahmadiawan, D., H. Abral, M. K. Ilham, P. Puspitasari, R. A. Nabawi, S. C. Shi, E. Sugiarti, et al. 2023. "Enhanced UV Blocking, Tensile and Thermal Properties of Bendable TEMPO-Oxidized Bacterial Cellulose Powder-Based Films Immersed in PVA/Uncaria Gambir/ZnO Solution." *Journal of Materials Research and Technology* 26:5566–5575. <https://doi.org/10.1016/j.jmrt.2023.08.267>.
- Rahmadiawan, D., H. Abral, R. A. Kotodeli, E. Sugiarti, A. N. Muslimin, R. I. Admi, A. Arafat, H.-J. Kim, S. M. Sapuan, and E. A. Kosasih. 2023. "A Novel Highly Conductive, Transparent, and Strong Pure-Cellulose Film from

- TEMPO-Oxidized Bacterial Cellulose by Increasing Sonication Power.” *Polymers* 15 (3): 643. <https://doi.org/10.3390/polym15030643>.
- Rahmadiawan, D., H. Abrial, R. M. Railis, I. C. Iby, M. Mahardika, D. Handayani, K. D. Natrana, D. Juliadmi, and F. Akbar. 2022. “The Enhanced Moisture Absorption and Tensile Strength of PVA/Uncaria Gambir Extract by Boric Acid as a Highly Moisture-Resistant, Anti-UV, and Strong Film for Food Packaging Applications.” *Journal of Composites Science* 6 (11): 337. <https://doi.org/10.3390/jcs6110337>.
- Rahmadiawan, D., Z. Fuadi, R. Kurniawan, H. Abrial, F. Ilhamsyah, A. Arafat, R. Rifelino, B. Syahri, and E. Indrawan. 2022. “Tribological Properties of Aqueous Carboxymethyl Cellulose/Uncaria Gambir Extract as Novel Anti-Corrosion Water-Based Lubricant.” *Tribology in Industry* 44 (4): 584–591. <https://doi.org/10.24874/TI.1357.08.22.10>.
- Saibuatong, O. A., and M. Phisalaphong. 2010. “Novo Aloe Vera-Bacterial Cellulose Composite Film from Biosynthesis.” *Carbohydrate Polymers* 79 (2): 455–460. <https://doi.org/10.1016/j.carbpol.2009.08.039>.
- Segal, L., J. J. Creely, A. E. Martin, and M. Conrad. 1958. “Empirical Method for Estimating the Degree of Crystallinity of Native Cellulose Using the X-Ray Diffractometer.” *Textile Research Journal* 29 (10): 786–794. <https://doi.org/10.1177/004051755902901003>.
- Sharif, S. N., N. Hashim, I. M. Isa, S. A. Bakar, M. I. Saidin, M. S. Ahmad, M. Mamat, M. Z. Hussein, and R. Zainul. 2021. “Polymeric Nanocomposite-Based Herbicide of Carboxymethyl Cellulose Coated-Zinc/aluminium Layered Double Hydroxide-Quinclorac: A Controlled Release Purpose for Agrochemicals.” *Journal of Polymers and the Environment* 29 (6): 1817–1834. <https://doi.org/10.1007/s10924-020-01997-0>.
- Sheng, J., T. Chen, R. Wang, Z. Zhang, F. Hua, and R. Yang. 2020. “Ultra-light cellulose nanofibril membrane for lithium-ion batteries.” *Journal of Membrane Science* 595 (September 2019): 117550. <https://doi.org/10.1016/j.memsci.2019.117550>.
- Siljander, S., P. Keinänen, A. Rätty, K. R. Ramakrishnan, S. Tuukkanen, V. Kunnari, A. Harlin, J. Vuorinen, and M. Kanerva. 2018. “Effect of Surfactant Type and Sonication Energy on the Electrical Conductivity Properties of Nanocellulose-CNT Nanocomposite Films.” *International Journal of Molecular Sciences* 19 (6): 1–14. <https://doi.org/10.3390/ijms19061819>.
- Song, J., C. Chen, S. Zhu, M. Zhu, J. Dai, U. Ray, Y. Li, et al. 2018. “Processing Bulk Natural Wood into a High-Performance Structural Material.” *Nature* 554 (7691): 224–228. <https://doi.org/10.1038/nature25476>.
- Tun, H. M., R. E. Wulansari, D. Pradhan, and Z. M. Naing. 2023. “Design, Fabrication and Measurement of Metal-Semiconductor Field Effect Transistor Based on Zinc Oxide Material.” *jerel* 2 (3): 104–111. <https://doi.org/10.58712/jerel.v2i3.103>.
- Udoetok, I. A., L. D. Wilson, and J. V. Headley. 2018. “Ultra-Sonication Assisted Cross-Linking of Cellulose Polymers.” *Ultrasonics Sonochemistry* 42 (October 2017): 567–576. <https://doi.org/10.1016/j.ultsonch.2017.12.017>.
- Ummartyotin, S., J. Juntaro, M. Sain, and H. Manuspiya. 2012. “Development of transparent bacterial cellulose nanocomposite film as substrate for flexible organic light emitting diode (OLED) display.” *Industrial Crops and Products* 35 (1): 92–97. <https://doi.org/10.1016/j.indcrop.2011.06.025>.
- Wu, C. N., and K. C. Cheng. 2017. “Strong, Thermal-Stable, Flexible, and Transparent Films by Self-Assembled TEMPO-Oxidized Bacterial Cellulose Nanofibers.” *Cellulose* 24 (1): 269–283. <https://doi.org/10.1007/s10570-016-1114-8>.
- Xi, J., Y. Lou, Y. Chu, L. Meng, H. Wei, H. Dai, Z. Xu, H. Xiao, and W. Wu. 2023. “High-flux bacterial cellulose ultrafiltration membrane with controllable pore structure.” *Colloids and Surfaces A: Physicochemical and Engineering Aspects* 656:130428. <https://doi.org/10.1016/j.colsurfa.2022.130428>.
- Ybañez, M. G., and D. H. Camacho. 2021. “Designing Hydrophobic Bacterial Cellulose Film Composites Assisted by Sound Waves.” *RSC Advances* 11 (52): 32873–32883. <https://doi.org/10.1039/d1ra02908h>.
- Yousefi, H., M. Faezipour, S. Hedjazi, M. M. Mousavi, Y. Azusa, and A. H. Heidari. 2013. “Comparative Study of Paper and Nanopaper Properties Prepared from Bacterial Cellulose Nanofibers and Fibers/Ground Cellulose Nanofibers of Canola Straw.” *Industrial Crops and Products* 43 (1): 732–737. <https://doi.org/10.1016/j.indcrop.2012.08.030>.
- Zhang, R., Y. Wang, D. Ma, S. Ahmed, W. Qin, and Y. Liu. 2019. “Effects of Ultrasonication Duration and Graphene Oxide and Nano-Zinc Oxide Contents on the Properties of Polyvinyl Alcohol Nanocomposites.” *Ultrasonics Sonochemistry* 59 (August): 104731. <https://doi.org/10.1016/j.ultsonch.2019.104731>.